ISSN 1054-660X, Laser Physics, 2007, Vol. 17, No. 8, pp. 1041–1052.




# Generation of an Electrical Signal upon the Interaction of Laser Radiation with Water Surface

**S. N. Andreev*, N. N. Il'ichev, K. N. Firsov, S. Yu. Kazantsev, I. G. Kononov, L. A. Kulevskii, and P. P. Pashinin**

*Prokhorov General Physics Institute, Russian Academy of Sciences, ul. Vavilova 38, Moscow, 119991 Russia*

*e-mail: andreevsn@ran.gpi.ru

Received January 22, 2007

**Abstract**—A new physical effect lying in the generation of an electrical signal (ES) upon the interaction of IR laser radiation with the water surface at a laser fluences lower than the plasma formation threshold is studied. An ES amplitude exceeding 15 V is detected. A one-to-one relationship between the observed effect and the bulk explosive boiling of water is established, and a qualitative interpretation is proposed. In the case of irradiation of an open surface, the ES is generated due to bulk explosive boiling accompanied by the evacuation and splashing of the surface layer, the destruction of the double electric layer on the surface, and the spread of an electrified vapor–drop mixture (balloelectric effect). When the surface is covered with a transparent plate, ES generation can be caused by the charge separation upon the detachment of the water surface from the plate by a vapor bubble resulting from boiling and the displacement of the charged water surface upon the expansion and contraction of the bubble.

PACS numbers: 52.38.Mf

**DOI:** 10.1134/S1054660X0708004X

## 1. INTRODUCTION

Many works are devoted to the study of the interaction of laser radiation with water (see [1–6] and references therein). The experiments are predominantly aimed at the analysis of the optical generation of sound, optical breakdown, and the propagation of light in liquid at relatively high laser flux densities. The effect of the electrical signal (ES) generation in the presence of a laser pulse incident on the water surface at a radiation energy density lower than the plasma formation threshold was observed for the first time in [7]. In the experiments from [7], a cell with water is placed in between the plates of an uncharged capacitor. When the water surface is irradiated with the pulse of an YSGG:$Cr^{3+}$:$Yb^{3+}$:$Ho^{3+}$ laser at wavelength $\lambda$ = 2.92 μm, a pulse energy of about 10 mJ, a pulse FWHM of about 150 ns, and the water absorption coefficient $k = 1.3 \times 10^4$ $cm^{-1}$, a potential difference with an amplitude of up to 10 mV is generated at the capacitor plates. In accordance with the interpretation from [7], the ES generation is caused by an increase in the degree of water dissociation in an overheated thin (about 1 μm) surface layer and the charge separation in this layer due to the difference of the $H^+$ and $OH^-$ diffusion coefficients. However, a comprehensive analysis and reliable interpretation of this effect were impeded by small ES amplitudes related to the relatively low energy of the laser radiation.

The first results on the ES generation upon the interaction of a high-power nonchain electrodischarge HF laser with water and several polar liquids can be found in [8]. The spectrum of this laser ($\lambda$ = 2.6–3.1 μm) exhibits lines with extremely high absorbances for hydroxyl-containing liquids (the absorbances are close to the absorbance at wavelength $\lambda$ = 2.92 μm of the YSGG:$Cr^{3+}$:$Yb^{3+}$:$Ho^{3+}$ laser). A relatively high (in comparison with the experiments from [7]) pulse energy of the HF laser ($E$ = 1.4 J) makes it possible to increase the ES signal by almost three orders of magnitude, which substantially facilitates the data acquisition needed for the interpretation of the phenomenon. When the open water surface is irradiated, the ES amplitude reaches a level of 6.5 V. When the water surface is covered with a plate made of fused silica, which is transparent in the IR range, the signal amplitude amounts to 5 V. In the experiments with polar hydroxyl-containing liquids (alcohols), only glycerol exhibits a significant ES signal. The experimental results from [8] made it possible to establish a relation of the ES generation upon the irradiation of the open water surface and bulk explosive boiling, which leads to the splashing of the surface layer and the spread of the resulting vapor–drop mixture. This enables one to qualitatively interpret the ES generation upon the interaction of laser radiation with the open water surface in terms of the well known balloelectric effect (water electrization upon its fragmentation, e.g., in waterfalls) [9–11] and to assume that the ES must be generated when the water surface is irradiated not only with 3-μm-range lasers but also with alternative lasers (e.g., $CO_2$ laser) whose pulse energy is higher than the threshold of bulk explosive boiling. Such unambiguous conclusions regarding the ES nature cannot be drawn based on the results from [8] in the case of irradiation of the covered water surface.

The purpose of this work is to further study ES generation for a water surface irradiated with a nonchain electrodischarge HF laser and to analyze the possibility of ES observation upon the irradiation of water by a TEA $CO_2$ laser. We compare the energy thresholds of the ES generation and bulk explosive boiling for both open and covered water surfaces irradiated with HF laser radiation. The nature of the phenomenon is qualitatively interpreted.

## 2. EXPERIMENTAL SETUP

In the experiments below, water is irradiated with two types of high-power lasers developed at the Prokhorov General Physics Institute, Russian Academy of Sciences: a nonchain electrodischarge HF laser and a TEA $CO_2$ laser. The HF laser, in which the chemical reaction is initiated by the self-sustained volume electrodischarge [12], has the active medium (a mixture of $SF_6$ and $C_2H_6$) with a volume of $8 \times 80 \times 80$ cm$^3$. The electrodischarge chamber is sealed with the $BaF_2$ plane-parallel plates mounted at an angle of incidence of about 15° relative to the optical axis. The external cavity with a length of 1.8 m is formed by plane aluminum and dielectric mirrors. In the working wavelength range $\lambda$ = 2.7–3.1 μm, the reflectance of the output dielectric mirror is 30%. To decrease beam divergence and to improve the laser beam quality in the cavity, we place apertures with a size of $75 \times 75$ mm in front of each mirror. In this configuration of the cavity, the HF laser energy is $E$ = 18 J. In the study of the interaction of the laser radiation with liquids when such high energies are unnecessary [13], the transverse size of the HF laser beam is decreased due to external apertures placed immediately behind the output cavity mirror. Under such conditions, the laser energy density distribution $W$, with respect to the radius $r$ of the focal spot at the surface of the object under study, can be well approximated with the Gaussian curve $W(r) = W_0\exp(-r^2/a^2)$. For a stationary position of the cell with water at the caustic of the focusing lens, the parameter $a$ ranges from 4.5 to 11 mm when the diameter of the external aperture ranges from 20 to 50 mm. In this case, the mean energy density in the spot $W_{av}$ weakly depends on parameter $a$. This makes it possible to trace the effect of the irradiation spot size on the ES characteristics at virtually constant $W_{av}$ at the water surface with a variation in the diameter of the external aperture. In the experiments below, the maximum energy of the HF laser is $E$ = 2.3 J for a pulse FWHM of 140 ns. The experiments are performed in the absence of the spectral selection of radiation.

In the measurements with the open water surface, the TEA $CO_2$ laser has a radiation pulse shape typical for such lasers: the first spike with a FWHM of 200 ns and a tail. The total pulse duration is 3 μs [14]. The central part of the output laser beam is cut with an aperture, and, then, the beam is focused on the water surface with a long-focal-length lens to a spot with a size of $20 \times 25$ mm. In the experiments, the maximum energy of the $CO_2$ laser radiation at the water surface is 17 J.

To attenuate the radiation of the HF and $CO_2$ lasers, we employ calibrated Teflon-film filters.

For the measurements, we predominantly employ distilled water with the resistivity $\rho \approx 10$ MΩ cm at a temperature of 20°C. In several experiments, we compare ESs using solutions of sodium chloride or drinking water containing various mineral salts.

We irradiate both the open water surface and the surface covered with an IR-transparent plate made of fused silica. Figure 1a demonstrates the experimental scheme for the open surface. A thin-wall aluminum cell with a diameter of 40 mm is filled with water and is placed at the surface of the lower plate of a plane capacitor. The laser radiation is deposited through a hole with a diameter of 80 mm in the upper plate. The plate diameter is 100 mm, and the thickness of the water layer in the cell is 8 mm (water reaches the cell edges). The distance $d$ from the water surface to the upper plate ranges from 0.8 to 12.8 cm. The signals from the capacitor plates are fed to the two-channel voltage repeater with a relatively high input resistance of the channels. Then, the signals are fed to a Tektronix TDS 220 two-channel digital oscilloscope. The potential difference at the plates (resulting ES) is obtained with the subtraction of signals at the second and first channels (CH2–CH1 mode).

The voltage repeater (Fig. 1b) is based on a 140UD18 chip.

In the experiments on the irradiation of the covered water surface, we only employ the HF laser. Figure 1c shows the measurement scheme. A plexiglass cell with an inner diameter of 30 mm and a depth of 10 mm is filled with water, is tightly covered with a fused-silica plate, and is placed between the capacitor plates. The plate is strongly pressed to the surface of the cell with a special flange. Otherwise, a pressure jump of up to 150 bar [13] at high energies of the HF laser leads to depressurization of the cell and the ejection of vapor, and gives rise to air bubbles under the surface of the quartz plate. Note that the ejection of vapor and the presence of air bubbles in water strongly affect the measured ES amplitude and shape. Water is irradiated through a hole with a diameter of 30 mm in the upper plate of the capacitor. The plate diameters are 60 mm. The ES measurements are performed in the same way as in the case of the open water surface.

The spread of the vapor–drop mixture emerging due to the laser pulse irradiation of the open water surface is controlled with the deflection of a He–Ne laser beam. For this purpose, a thin (with a diameter of about 1 mm) beam of a He–Ne laser passes under the upper plate of the capacitor and strikes the photodiode (Fig. 1d). Figure 2 shows a typical oscillogram of the photodiode signal. When the laser beam is crossed by the front of the vapor–drop mixture, the photodiode signal significantly decreases due to the optical perturbation. This makes it possible to measure the time at which the front

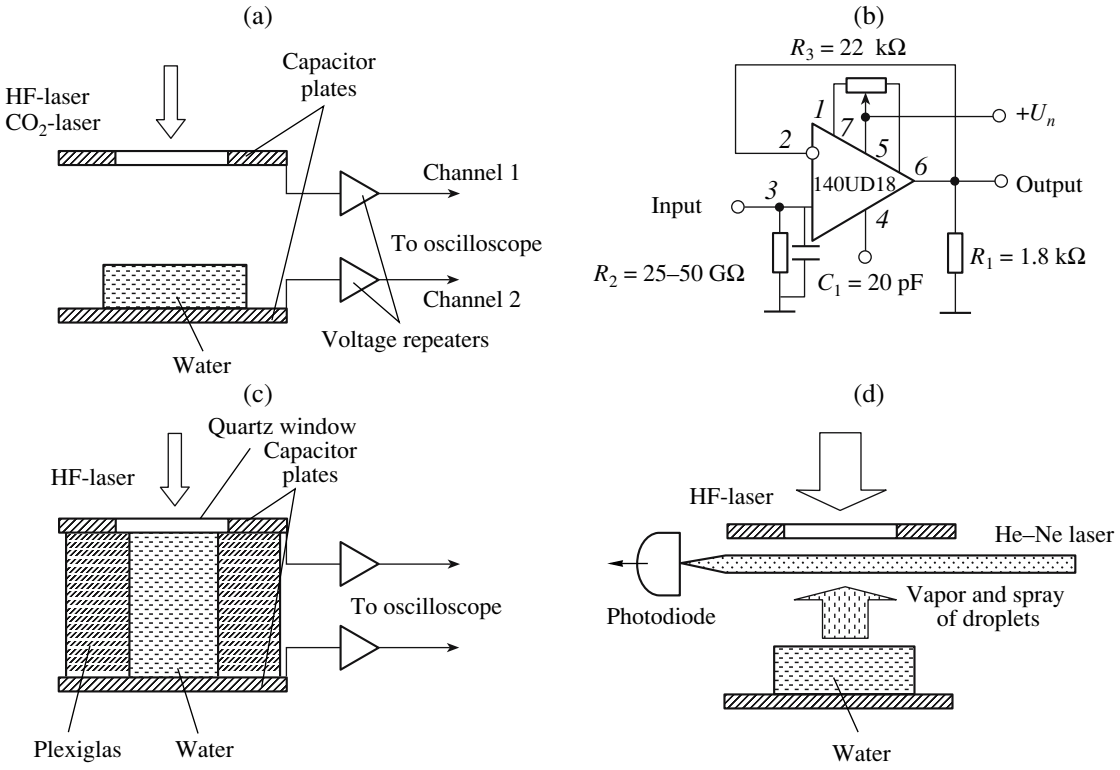


**Fig. 1.** Scheme of the experimental setup: (a) open water surface, (b) electric circuit of the voltage repeater, (c) covered water surface, and (d) scheme for the measurement of the time of the vapor–drop mixture spread.

reaches the upper plate. The time counted from the beginning of the laser pulse to the moment of the recovery of the stationary amplitude in the photodiode signal corresponds to the total time during which the vapor–drop mixture moves inside the capacitor.

In the above analysis of the results from [8], we mention the relation of the ES generation upon the irradiation of the open water surface and bulk explosive boiling. In this work, we determine the thresholds of bulk explosive boiling using the radiation energy of the HF laser at the open and covered water surfaces. For this purpose, we employ a piezoelectric pressure transducer based on a thin PVDF film with an area of 3.1 $cm^2$ developed and calibrated at the Laser Optoacoustic Laboratory, International Laser Center, Moscow State University (see [13] for the details of such measurements). In this work, the purpose of the measurements is to compare the energy thresholds of bulk explosive boiling and ES generation under identical conditions for laser focusing.

## 3. EXPERIMENTAL RESULTS AND DISCUSSION

### *3.1. Open Water Surface*

Figure 3 demonstrates typical ES oscillograms for the interaction of the HF laser radiation with the open water surface measured at various values of parameter $a$ and almost equal mean energy densities $W_{av}$ in the irradiation region. We see that the signal contains a relatively short first spike and a slowly increasing second component. Both the first spike and the second component substantially increase with increasing $a$ (i.e., with increasing area of irradiated surface and, hence, the energy of irradiating pulse). This tendency is main-

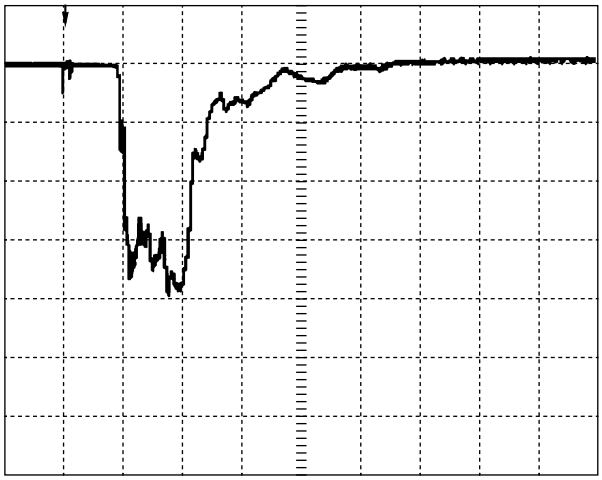

**Fig. 2.** Typical oscillogram of the photodiode signal obtained for the HF laser irradiation of the open water surface at $E$ = 0.7 J, $d$ = 2.1 cm, and $a$ = 6 mm. The vertical and horizontal scales are 50 mV/div and 500 μs/div, respectively. The arrow shows the position of the laser pulse.

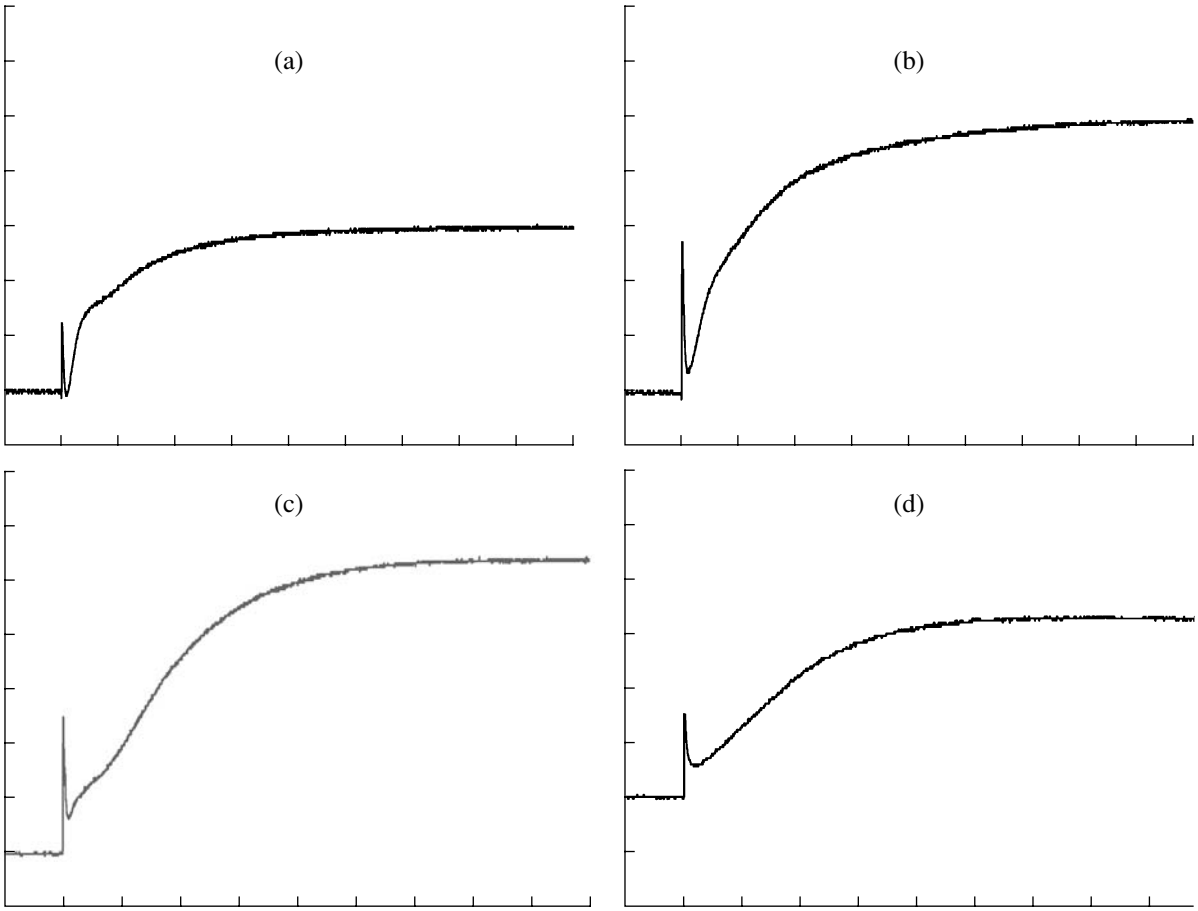


**Fig. 3.** ES oscillograms obtained for the HF laser irradiation of an open water surface at (a) $E = 0.4$ J, $a = 4.5$ mm, and a vertical scale of 1 V/div; (b) $E = 0.87$ J, $a = 6.5$ mm, and a vertical scale of 1 V/div; (c) $E = 1.5$ J, $a = 8.5$ mm, and a vertical scale of 2 V/div; (d) $E = 2.3$ J, $a = 11$ mm, and a vertical scale of 5 V/div; a horizontal scale of 500 μs/div; and $d = 19$ mm.

tained at smaller values of $W_{av}$ in the irradiation region down to the threshold level. It is seen from Fig. 3d that the amplitude of the second maximum amounts to $U = 16.3$ V at $a = 11$ mm. The amplitude ratio $\delta$ of the first and second maxima weakly depends on $a$ at constant $W_{av}$, and decreases with decreasing laser energy $E$ at a given $a$.

Figure 4 shows the ocillograms of ES and the laser pulse. When these oscillograms were recorded, the upper plate of the capacitor was grounded and the signal from the lower plate was directly fed to the oscilloscope input in the absence of the voltage repeater. It is seen that the ES emerges at the leading edge of the laser pulse. The duration of the leading edge of the first spike ranges from 4 to 7 μs and depends on $a$, whereas the duration of the trailing edge at half amplitude is $\tau \approx 17$ μs at the maximum (in this experiment) value $W_{av} = 0.66$ J/cm$^2$. When $W_{av}$ decreases, $\tau$ also decreases and reaches a level of 5 μs at $W_{av} = 0.23$ J/cm$^2$. The value of $\tau$ cannot be determined at $W_{av} \le 0.2$ J/cm$^2$ in the vicinity of the threshold of the effect due to a variation in the ES shape. The problem of the variation in the ES shape in the near-threshold region is beyond the scope of this work and will be analyzed in future publications.

The duration $\tau_f$ of the leading edge of the slowly increasing ES component depends on both distance $d$ from the water surface to the upper plate of the capacitor and laser pulse energy $E$: it increases with increasing $d$ and decreasing $E$ in the region $W_{av} \ge 0.2$ J/cm$^2$. The measurements performed at various $E$, $d$, and $a$ show that the value of $\tau_f$ well correlates with the time over which the motion (spread) of the vapor–drop mixture takes place inside the capacitor. Recall that this time is measured using the deflection of the He–Ne laser beam (Figs. 1d and 2). Thus, an increase in ES, after the first relatively short spike, can be related to the spread of the vapor–drop mixture caused by the laser irradiation of the surface. Hence, the vapor–drop mixture provides for the charge transfer and an increase in the amplitude of the second ES maximum with an increase in the irradiated water surface area (Fig. 3) (i.e., with an increase in $E$ at constant $W_{av}$) is related to an increase in this charge. For the conditions of Fig. 3d, simple estimates yield the charge $q \approx 2.2 \times 10^{-10}$ C transferred by the vapor–drop mixture with regard to

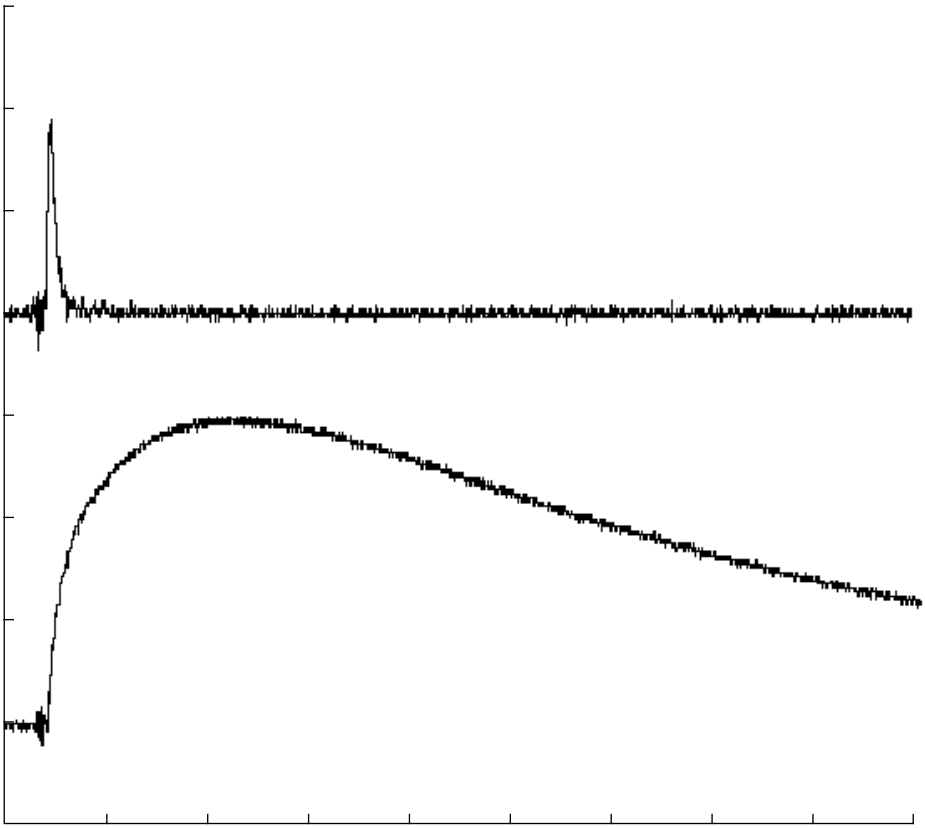

**Fig. 4.** Oscillograms of (upper curve) laser pulse with a vertical scale of 100 mV/div and (lower curve) ES with a vertical scale of 200 mV/div obtained for the HF laser irradiation of the open water surface at $E = 0.87$ J, $d = 19$ mm, $a = 6.5$ mm, and a horizontal scale of 2.5 μs/div.

the capacitance at each input of the voltage repeater (Fig. 1b) $C_1 = 20$ pF and the capacitance $C \approx 4$ pF of the capacitor with the cell filled with water.

Figure 5 shows the dependences of the amplitude of the second ES maximum $U$ and the value of $\tau_f$ at a level of 0.9 $U$ on $E$ obtained for $a = 6.5$ mm and $d = 19$ mm. Figure 6 shows the dependence of the amplitude $U_1$ of the first maximum on $E$ for the same values of $d$ and $a$. It is seen from Figs. 5 and 6 that the scatters of dots on curves $U$ and $U_1$ are relatively large. This is clearly seen in Fig. 5, where the intervals of $U$ in the measurements performed over five days are demonstrated for several values of $E$. The dots on the curves in Fig. 5 correspond to the series in which the duration $\tau_f$ of the leading edge of the second ES component is controlled. Note that the scatter with respect to $\tau_f$ is smaller. In general, the reasons for such a large scatter of the values of $U$ remain unclear. One of the possible factors that can affect the value of $U$ even in a single experimental series (about 20 points) is the presence of dust particles in the ambient air. These particles are charged due to the corona effect in the high-voltage modules of the HF laser. Obviously, the ES is varied if such particles are drawn by the spreading vapor–drop mixture. In spite of a relatively large scatter of the data presented in Figs. 5 and 6, we observe a general tendency towards an increase in $U$ and $U_1$ with an increase in $E$, such that $U$ and $U_1$ become substantially different from zero at $E \geq 0.15$ and 0.21 J, respectively. Hence, the energy thresholds of the first and second ES components are slightly different. However, allowing for the scatter of data, we do not analyze this effect. It also follows from the comparison of curves $U(E)$ and $U_1(E)$ that, as was mentioned, the ratio $\delta = U_1/U$ increases with increasing $E$. The duration $\tau_f$ of the leading edge of the second ES component exhibits a maximum at $E \approx 0.26$ J (Fig. 5). Evidently, a decrease in $\tau_f$ with increasing $E$ at $E > 0.26$ J is related to an increase in the velocity of the spreading vapor–drop mixture. The reason for a decrease in this parameter with decreasing $E$ in the range $E < 0.26$ J remains unclear.

The above experimental data make it possible to qualitatively interpret the ES nature in the case of the laser irradiation of the open water surface.

(i) As was mentioned, the ES characteristics correlate with the spread of the vapor–drop mixture in the gap between the capacitor plates. It is known that the ejection of the vapor–drop jet is caused by the bulk explosive boiling of liquid, which has a threshold with respect to the laser energy density [5, 6, 15]. In a spite of a small (about 1 μm) penetration depth of the 3-μm radiation in water, the maximum of the laser-induced

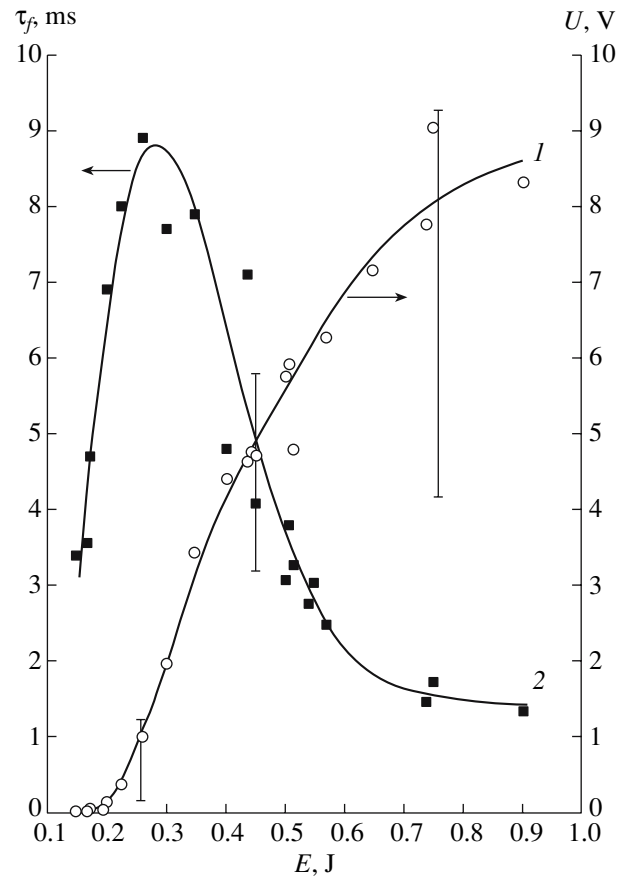


**Fig. 5.** Plots of (*1*) amplitude $U$ and (*2*) duration of the leading edge $\tau_f$ at a level of 0.9 $U$ for the second ES component vs. the HF laser radiation energy $E$ for the open water surface at $d$ = 19 mm and $a$ = 6.5 mm.

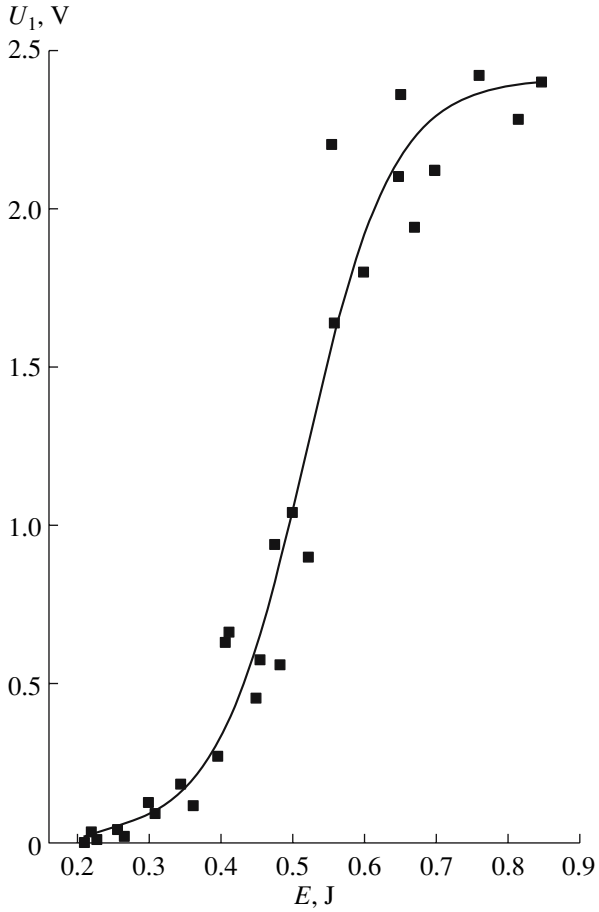


**Fig. 6.** Plot of the amplitude $U_1$ of the first ES maximum vs. the HF laser radiation energy $E$ for the open water surface at $d$ = 19 mm and $a$ = 6.5 mm.

temperature profile is shifted from the surface towards the depth of liquid [6]. Therefore, when the temperature of the limiting overheating (spinodal) is reached, the boiling is induced under the surface layer. This leads to the detachment of the surface layer [6] and its spread (sputtering) as the vapor–drop mixture.

If ES generation is related to bulk explosive boiling, these effects must exhibit nearly equal laser-energy thresholds under identical conditions for beam focusing. Figure 7 shows the dependence of the pressure pulse amplitude $P_0$ generated due to the interaction of the HF laser radiation with the open water surface and the duration $\tau_p$ of the trailing edge of the pressure pulse at a level of $0.5P_0$ on $E$ measured with the pressure transducer under the same focusing conditions as in Figs. 5 and 6 ($a$ = 6.5 mm). It follows form Fig. 7 that, in the range $E \le 0.21$ J, quantity $\tau_p$ remains constant within the experimental error. At $E \approx 0.21$ J, the curve $\tau_p(E)$ exhibits a breakpoint. In accordance with [13], this indicates the beginning of the bulk explosive boiling of water. In the range $E \approx 0.21$ J, $\tau_p$ decreases with increasing $E$. Thus, we can assume that the explosive boiling threshold is $E = E_{th}^0 \ge 0.21$ J. The comparison of the data presented in Figs. 5 and 6 shows that the $E$ values corresponding to the beginning of a significant increase in ES are really close to $E_{th}^0$.

It is also known that the surface layer of polar liquids (in particular, water) is spontaneously polarized [9]. We can assume that the first rapidly increasing ES spike, which starts at the leading edge of the laser pulse, is related to the destruction of the surface double electric layer upon bulk explosive boiling and its recovery upon water cooling and the termination of boiling. The calculations with the model from [15] at $W_{av}$ = 0.66 J/cm$^2$ (the conditions of Fig. 3) yield an estimate for the time of water surface cooling to room temperature after the explosion about 50 μs. This time is close to the duration of the trailing edge of the ES spike (Fig. 3). Note that this interpretation of the first ES spike is hypothetical. For a reliable interpretation of the nature of the first ES spike, we need to further study ES generation upon the interaction of laser radiation with water and other polar liquids.

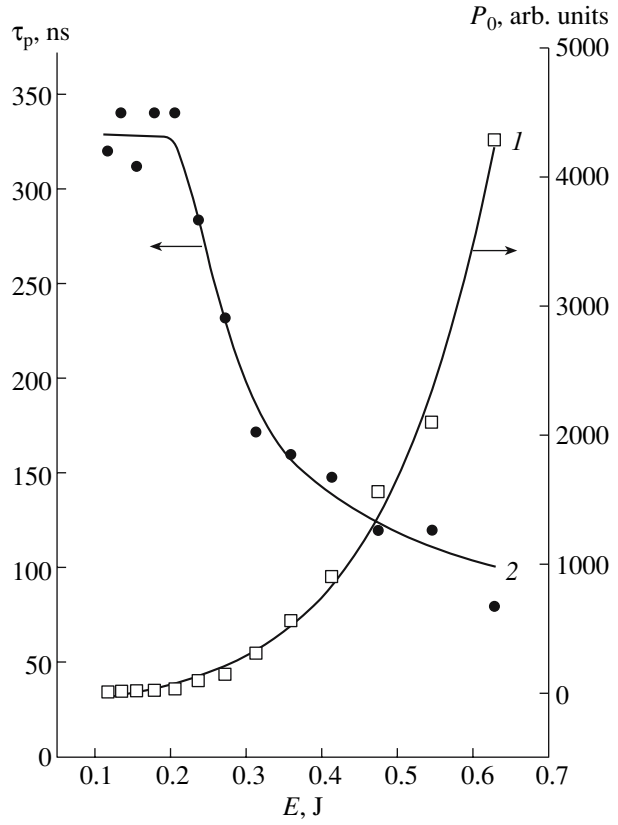


**Fig. 7.** Plots of (*1*) amplitude $P_0$ and (*2*) duration of the trailing edge $\tau_p$ at a level of $0.5P_0$ for the pressure signal vs. the HF laser radiation energy $E$ for the open water surface at $a = 6.5$ mm.

(ii) It follows from the above data that the vapor–drop mixture resulting from bulk explosive boiling and the detachment (sputtering) of the surface water layer is involved in the charge transfer. Recall the known balloelectric effect [9–11] lying in the electrization of water and other polar liquids upon sputtering (fragmentation). We can assume that, in the case under study, the charge transferred between the capacitor plates emerges due to the balloelectric effect. This interpretation is proven by the ES sign in the oscillograms presented in Figs. 3 and 4. The potential difference at the capacitor plates results from the subtraction of the signal in the first channel of the oscilloscope from the signal in the second channel (Fig. 1a). Therefore, the positive ES indicates the motion of a negative charge inside the capacitor, which is typical of the balloelectric effect upon the sputtering of pure water with the formation of small droplets [10]. In the presence of impurities, the balloelectric effect in water becomes weaker [10], which is also observed in the experiments. By way of example, Fig. 8 shows the ES oscillograms recorded at various concentrations $K$ of sodium chloride in water. It is seen that an increase in the salt concentration leads to a decrease in the ES amplitude and, even its sign reversal at relatively high $K$.

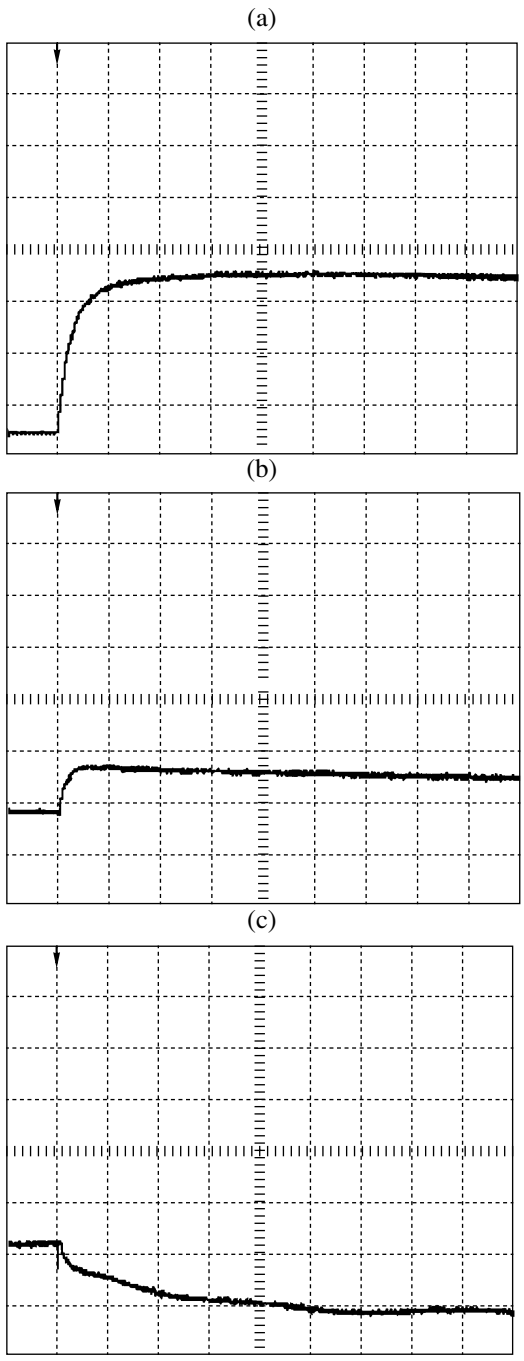


**Fig. 8.** ES oscillograms recorded at various concentrations $K$ of sodium chloride in water obtained for the HF laser irradiation of the open water surface at $E = 0.65$ J, $a = 6$ mm, and $d = 6$ cm: (a) $K = 0$ (vertical and horizontal scales are 500 mV/div and 5 ms/div, respectively); (b) $K = 5 \times 10^{-5}$ mol/l (vertical and horizontal scales are 500 mV/div and 10 ms/div, respectively); and (c) $K = 0.1$ mol/l (vertical and horizontal scales are 50 mV/div and 5 ms/div, respectively).

As was expected, ES is also generated when the open water surface is irradiated by a pulsed $CO_2$ laser, provided that the laser energy density exceeds the threshold of bulk explosive boiling and the vapor–drop

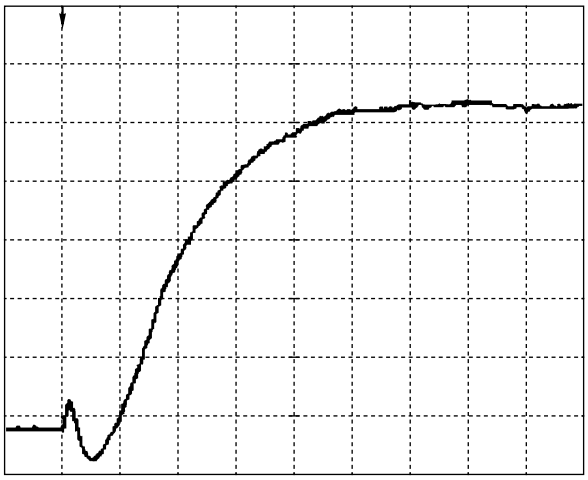

**Fig. 9.** ES oscillogram obtained for the $CO_2$ laser irradiation of the open water surface at $E = 7.8$ J, $d = 19$ mm, a vertical scale of 1 V/div, and a horizontal scale of 100 μs/div.

mixture is ejected. Figure 9 demonstrates the ES oscillogram recorded at the $CO_2$ laser energy $E = 7.8$ J and $d = 19$ mm. It is seen that, in contrast to the oscillograms presented in Fig. 3, the first relatively short ES component exhibits a fragment with negative polarity and that the duration $\tau_f$ of the leading edge of the second component, which is determined by the velocity of the spreading vapor–drop mixture, is significantly shorter than that in Fig. 3. Note that a less developed fragment of negative polarity was also observed for the first ES component in the experiments with the HF laser in a narrow range of the laser energy density: $W_{av} = 0.34$–$0.42$ J/cm$^2$. In general, the ESs generated due to the interaction of the HF and $CO_2$ laser radiation with the open water surface are similar.

Thus, based on the above data, we can interpret the ES generation upon the interaction of the laser radiation with the open surface in terms of the explosive boiling of water, the sputtering of its surface layer, the destruction of the surface double electric layer, and the spread of the electrified vapor–drop mixture (balloelectric effect).

### *3.2. Covered Water Surface*

Figure 10 demonstrates typical ES oscillograms recorded upon the interaction of HF laser radiation with the covered water surface at the mean energy density $W_{av} = 0.6$ J/cm$^2$ and various values of parameter $a$. Figure 11 shows the ES and laser pulse oscillograms obtained for the same $W_{av}$ and $a = 8.5$ mm (these measurements, the upper plate of the capacitor was grounded). It follows from Fig. 10 that, in contrast to the open surface, the ES signal is not unipolar. The amplitude $U^-$ of the negative component is virtually independent of $a$, whereas the amplitude $U^+$ of the positive component increases with increasing $a$. The first

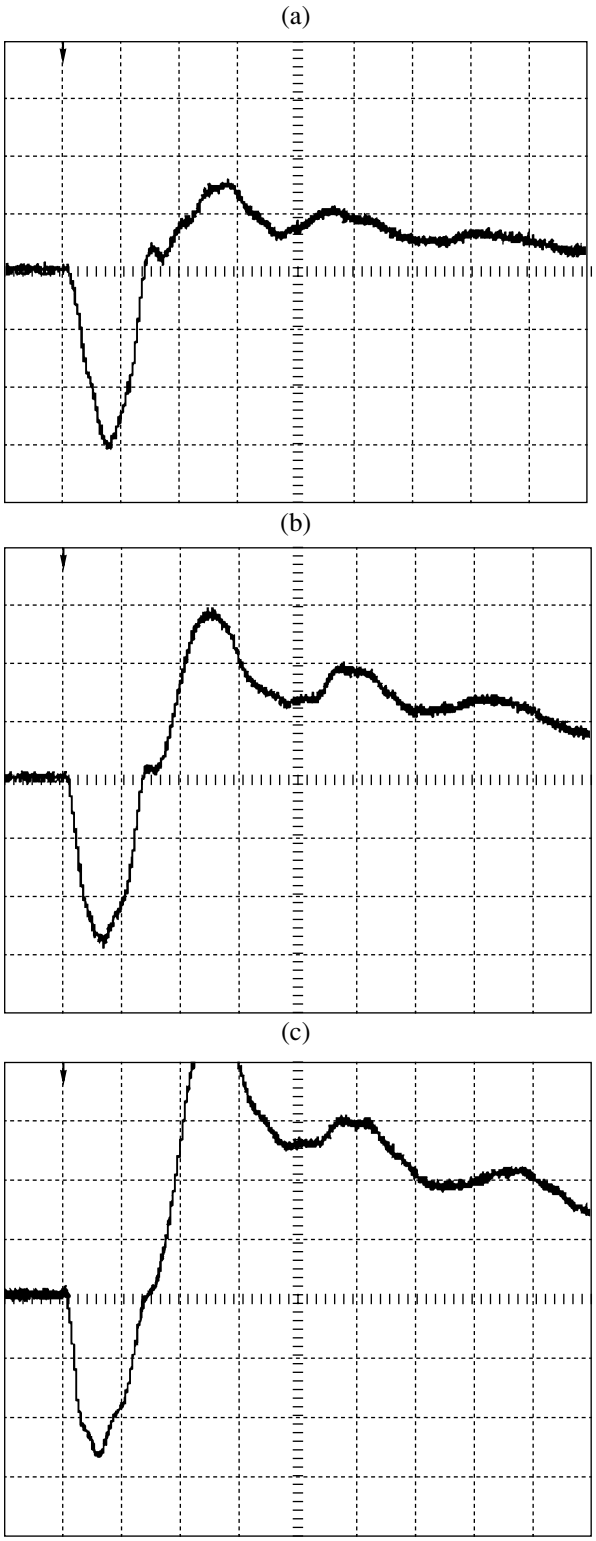


**Fig. 10.** ES oscillograms obtained for the HF laser irradiation of the covered water surface at a vertical scale of 2 V/div, a horizontal scale of 100 μs/div, $W_{av} = 0.6$ J/cm$^2$, and $a$ = (a) 4.5, (b) 6.5, and (c) 8.5 mm.

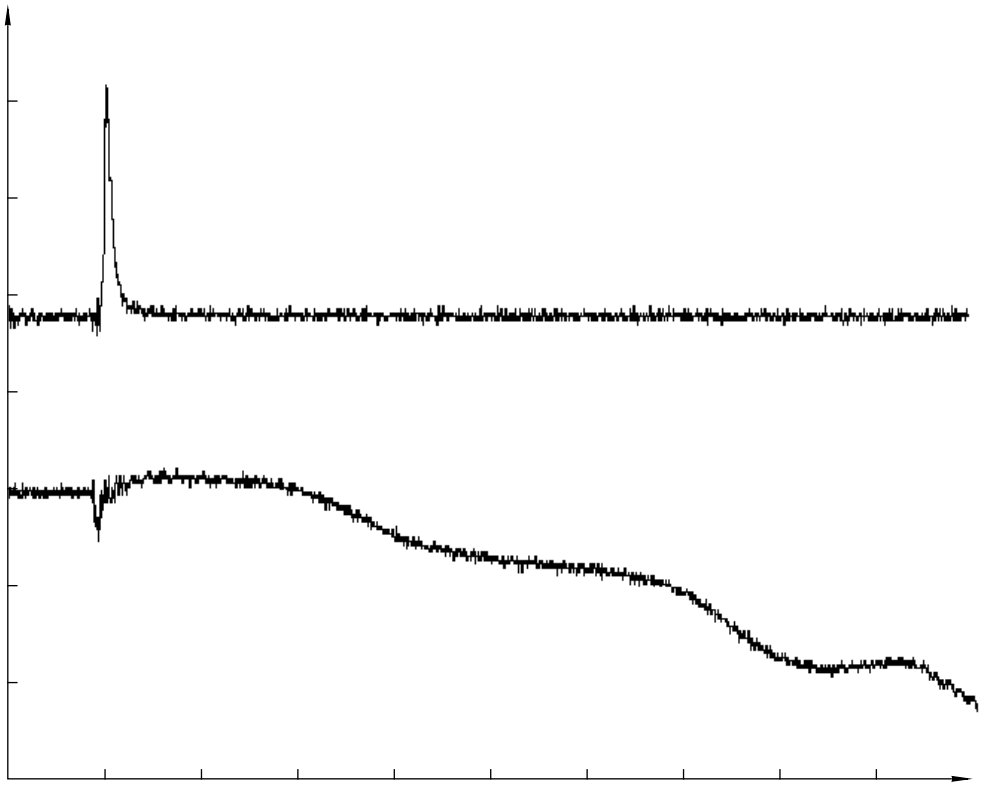

**Fig. 11.** Oscillograms of (upper curve) laser pulse with a vertical scale of 100 mV/div and (lower curve) ES with a vertical scale of 500 mV/div obtained for covered water surface at $W_{av} = 0.6$ J/cm$^2$ and a horizontal scale of 2.5 μs/div.

(negative) ES maximum is reached with a relatively large delay relative to the laser pulse $\Delta t$ = 74–82 μs depending on $a$. It follows from the calculation using the model from [15] that water is cooled to a temperature of about 40°C over this time. It is seen from Fig. 11 that, in the beginning, at a relatively short (about 5 μs) fragment, the ES is positive and its magnitude is significantly lower than $U^-$.

Figures 12 and 13 demonstrate the dependences of the amplitudes of the negative $U^-$ and positive $U^+$ ES components on HF laser energy $E$ for the parameter $a$ = 8.5 mm. It is seen that the ES generation threshold is $E \approx 0.21$ J. For the laser pulse energies $E \le 0.76$ J, we have $U^- > U^+$. At higher energies, the amplitude of the positive ES component exceeds the negative amplitude and amounts to $U^+ \approx 13$ V at $E = 1.2$ J. Note that the scatter of points on the dependence $U^+(E)$ is significantly greater than that for $U^-(E)$.

By analogy with [16, 17], we assume in [8] that ES generation when the covered water surface is irradiated with HF laser radiation can be related to the excitation (destruction) of the double electric layers in the presence of the acoustic wave generated due to the laser-induced heating of a thin water layer. We also mention the inconsistencies of this interpretation: in particular, the oscillation periods in the ES oscillograms (Figs. 10 and 11) do not correlate with the double pass time of the acoustic wave $T_s = 2L/V_s$ in the cell with water ($L$ is the water layer thickness and $V_s$ is the speed of sound). In this work, we have $T_s = 13.3$ μs. In the framework of the interpretation, we fail to account for the large time delay $\Delta t$ = 74–82 μs (Fig. 10) of the first (negative) ES maximum relative to the laser pulse, since the acoustic wave decays over this time due to diffraction and reflec-

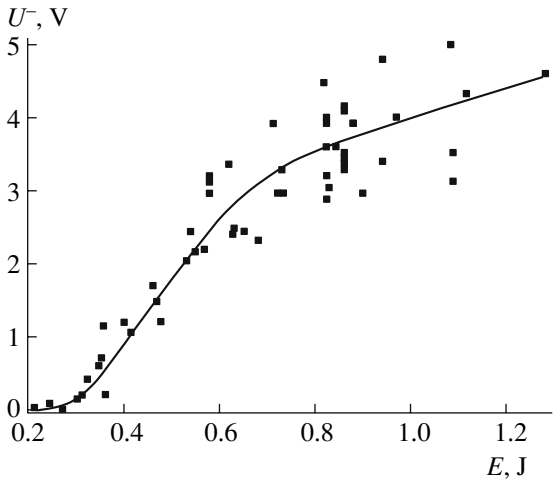


**Fig. 12.** Plot of the amplitude $U^-$ of the negative ES component vs. the HF laser radiation energy $E$ for the covered water surface at $a$ = 8.5 mm.

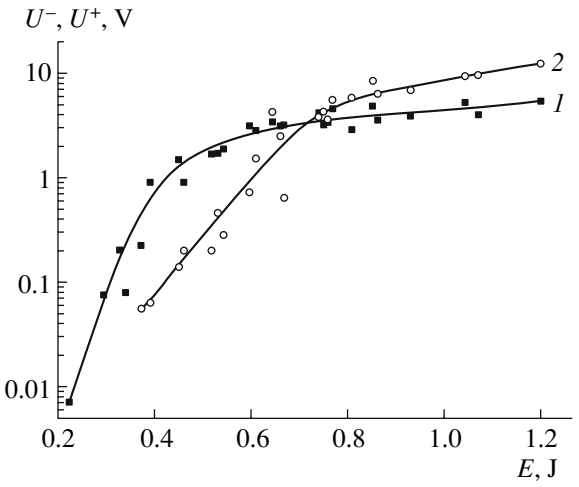


**Fig. 13.** Plots of the amplitudes of (*1*) negative $U^-$ and (*2*) positive $U^+$ ES components vs. the HF laser radiation energy $E$ for the covered water surface at $a$ = 8.5 mm.

tions from the cell surfaces and quartz window. Note that, in the case of the acoustic excitation of double electric layers in composites (e.g., concrete [18]), the measured ES amplitudes are three orders of magnitude lower than the amplitudes from [8] and this work. (We do not consider the emf generation upon the compression of polar isolators in the presence of shock waves with a pressure higher than $10^5$ bar at the wave front [19]. In [8] and in this work, the maximum laser-induced pressure in a cell with water is no greater than 150 bar.) These contradictions necessitate a search for alternative mechanisms for ES generation upon the laser heating of water surface. First, we must interpret the charge separation in the system under study.

Recall the known effect of the electrization of newly formed surfaces, including the surfaces resulting from the creation of cavitation bubbles (see [20–22] and references therein). We can assume that, in the case under study, the electrization is caused by the formation of a vapor bubble under the surface of the quartz window. The bubble is formed at a relatively high laser energy density owing to the explosive boiling of water in the strongly overheated thin surface layer [13, 15]. When the bubble emerges, the water surface is detached from the surface of the quartz window, which presumably leads to a charge separation. The ES generation must be related to the motion of the charged liquid interface upon the expansion and subsequent contraction (upon cooling) of the vapor bubble. The validity of this hypothesis is proven by the study of the evolution of bubbles when the covered toluene surface is irradiated with a KrF laser (the radiation absorption coefficient is $K \approx 1.1 \times 10^3$ cm$^{-1}$) [23]. This study shows that the maximum size (about 0.4 mm along the optical axis) of the expanding vapor bubble is reached with a delay of 50–60 μs relative to the surface irradiation with the laser pulse. This delay is close to the delay of the first (negative) ES maximum (Fig. 10).

Thus, in the case of the laser irradiation of a covered surface, it might be supposed that ES generation can be interpreted using the charge separation that must be related to the detachment of the water surface from the surface of the quartz window upon the formation of the vapor bubble due to the explosive boiling of water and the subsequent motion of the charged water surface upon the expansion and contraction of the vapor bubble. However, in the framework of this approach, we need to prove that the ES generation and explosive boiling thresholds, with respect to the laser radiation energy, are close to each other. For this purpose, we measure the explosive boiling threshold under the same focusing conditions as in the measurements of the curves $U^-(E)$ and $U^+(E)$ (Figs. 12 and 13) (the parameter $a$ is 8.5 mm). The details of such measurements can be found in [13]. For the convenience of the further analysis, we briefly characterize the corresponding procedure. Figure 14 demonstrates a typical shape for pressure signal $P$ measured with the pressure transducer upon irradiation of the covered water surface with HF laser radiation when the laser radiation energy exceeds the bulk boiling threshold. The signal (inset in Fig. 14) exhibits two pressure maxima: the first (photoacoustic) maximum $P_c$ is related to the laser-induced thermal expansion of water and the second one $P_c^{eb}$ is related to water boiling. When the laser energy $E$ increases, the time interval between the maxima decreases and $P_c^{eb}$ increases faster than $P_c$ does. Finally, at high laser energies, the pressure pulse amplitude is determined by boiling process. The energy dependence of $P_c^{eb}$ makes it possible to determine the explosive boiling threshold. Figure 14 shows the dependences of $P_c^{eb}$ and $P_c$ on $E$ measured at $a$ = 8.5 mm. It follows from a comparison of Figs. 12 and 13 with Fig. 14 that the ES generation and bulk explosive boiling thresholds are close to each other within the experimental accuracy.

Thus, the results presented unambiguously indicate a relation between ES generation upon the laser irradiation of covered (and open) surface and the bulk explosive boiling of water (i.e., the formation of a vapor bubble under the surface of a quartz window). Based on this conclusion, we propose the following simplified model of ES generation. We assume that the charge separation results from the detachment of the water surface from the surface of the quartz window owing to the vapor bubble and that charge $q$ does not dissipate during the evolution of the bubble. With regard to relatively large irradiation spots, we consider the bubble as a plane capacitor with constant plate area $S$ and distance $d$ that is varied with time. In a rough approximation, we assume that the measured ES ($U_{ES}$) is proportional to

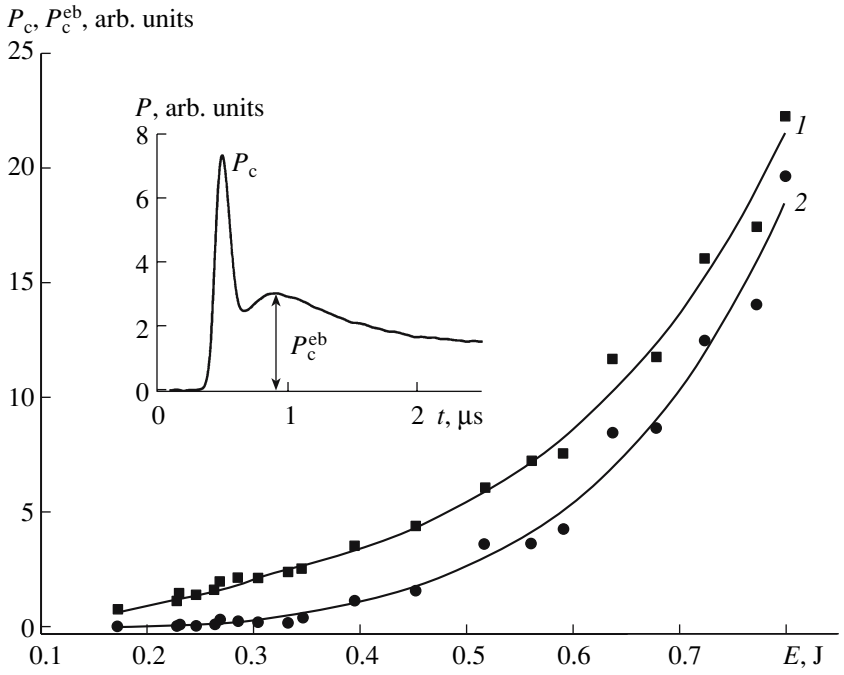


**Fig. 14.** Plots of (*1*) $P_c$ and (*2*) $P_c^{eb}$ pressure amplitudes vs. the HF laser radiation energy $E$ for the covered water surface at $a$ = 8.5 mm. The inset shows the pressure pulse shape.

the potential difference $\tilde{U}$ across the bubble-capacitor. Then, we obtain $\tilde{U} \sim d$ and $U_{ES} = \text{const}\,d$ due to the fact that $\tilde{U} = q/c$ ($c$ is the capacitance of the bubble-capacitor), $q \sim S$, and $c \sim S$. Thus, the ES value only depends on $d$ and appears independent of the irradiation spot area $S$. The maximum ES corresponds to the maximum expansion of the bubble (in the direction of the laser beam). Then, the signal must decrease upon the compression of the bubble with vapor cooling. In the first approximation, this rough capacitor model makes it possible to interpret the long delay of the first (negative) ES pulse relative to the laser pulse (Fig. 10) and the weak dependence of the amplitude of the negative component $U^-$ on the irradiation spot size. However, the model does not allow the experimentally observed time variation of the ES polarity to be interpreted. Apparently, an adequate model of ES generation must be based on the study of vapor bubble(s) evolution in the presence of large irradiation spots and a thorough analysis of the ES detection system. Note that a relatively high conductance of distilled water (the resistance of water in the cell is about 1.6 MΩ) must be taken into account. Presumably, the ES characteristics can be varied when the opposite (with respect to the irradiation) water surface is free, for example, in the case of irradiation through a window at the bottom and the open upper surface [23].

Finally, note that, similarly to the scenario realized for the open surface, the ES amplitude and shape are strongly affected by impurities. Specifically, the substitution of tap water or drinking water with a salt content of about 500 mg/l for distilled water causes a significant decrease in the amplitude and a polarity reversal of the measured ES.

## CONCLUSIONS

Thus, the nature of the electrical signal generated upon the interaction of the IR laser radiation with the water surface is studied for the energy laser fluences lower than the plasma formation threshold. The measured ES amplitudes are higher than 10 V. The dependences of the ES amplitudes on the laser radiation energy are obtained. The thresholds of the bulk explosive boiling of water are measured for the same focusing conditions. A one-to-one relationship between ES generation and the bulk explosive boiling of water is demonstrated. The following qualitative interpretation is proposed. In the case of the irradiation of an open surface, the ES is generated due to the bulk explosive boiling of water that is accompanied by the detachment and sputtering of its surface layer, a violation of the double electric layer on the surface, and the spread of the electrified vapor–drop mixture (balloelectric effect). When the irradiated surface is covered with a transparent plate, ES generation can be due to the charge separation upon the detachment of the water surface from the plate surface in the presence of a vapor bubble that results from bulk explosive boiling and the motion of the charged water surface upon the expansion and contraction of the vapor bubble. Finally, note the

qualitative character of this interpretation. It is expedient to continue experimental and theoretical study aiming at the construction of quantitative models.

## ACKNOWLEDGMENTS

This work was supported by the Russian Foundation for Basic Research (project nos. 06-02-08032-ofi, 05-08-33704, and 06-02-16779) and the Russian Science Support Foundation.

## REFERENCES

1. G. A. Askar'yan, A. M. Prokhorov, G. F. Chanturiya, and G. P. Shipulo, Zh. Eksp. Teor. Fiz. **44**, 2180 (1963) [Sov. Phys. JETP **17**, 1463 (1963)].
2. K. L. Vodop'yanov, L. A. Kulevskii, P. P. Pashinin, and A. M. Prokhorov, Zh. Eksp. Teor. Fiz. **82**, 1820 (1982) [Sov. Phys. JETP **55**, 1049 (1982)].
3. K. L. Vodop'yanov, L. A. Kulevskii, V. G. Mikhalevich, and A. M. Rodin, Zh. Eksp. Teor. Fiz. **91**, 114 (1986) [Sov. Phys. JETP **64**, 81 (1982)].
4. V. G. Mikhalevich and A. M. Rodin, Sudostr. Promyshl., Ser. Akust., No. 2, 105 (1987) [in Russian].
5. A. F. Vitshas, L. M. Dorozhkin, V. S. Doroshenko, et al., Akust. Zh. **34**, 437 (1988) [Sov. Phys. Acoust. **34**, 254 (1988)].
6. S. N. Andreev, I. N. Kartashov, and A. A. Samokhin, Kratk. Soobshch. Fiz., No. 6, 10 (2003) [in Russian].
7. N. N. Il'ichev, L. A. Kulevskii, and P. P. Pashinin, Quantum Electron. **35**, 959 (2005).
8. S. N. Andreev, N. N. Il'ichev, S. Yu. Kazantsev, et al., Elektron. Zh. "Issled. Ross." **9** (094), 892, (2006) [in Russian]; http://zhurnal.ape.relarn.ru/articles/2006/094.pdf.
9. R. R. Salem, *Theory of Double Layer* (Fizmatlit, Moscow, 2003) [in Russian].
10. V. I. Arabadzhi, *Puzzles of Simple Water* (Znanie, Moscow, 1973) [in Russian].
11. Ya. E. Geguzin, *Drop* (Nauka, Moscow, 1973) [in Russian].
12. A. A. Belevtsev and K. N. Firsov, *Encyclopedia of Low-temperature Plasma*, Vol. XI-4: *Gas and Plasma Lasers* (Fizmatlit, Moscow, 2005), p. 761 [in Russian].
13. S. N. Andreev, K. N. Firsov, I. G. Kononov, and A. A. Samokhin, Proc. SPIE **6161**, 616104 (2006).
14. A. A. Belevtsev, K. N. Firsov, S. Yu. Kazantsev, and I. G. Kononov, Appl. Phys. B **82**, 455 (2006).
15. S. N. Andreev, S. V. Orlov, and A. A. Samokhin, Tr. Inst. Obshch. Fiz., Ross. Akad. Nauk **60**, 127 (2004) [in Russian].
16. T. V. Fursa, A. V. Savel'ev, and K. Yu. Osipov, Zh. Tekh. Fiz. **73** (11), 59 (2003) [Tech. Phys. **48**, 1419 (2003)].
17. T. V. Fursa, N. N. Khorsov, and E. A. Baturin, Zh. Tekh. Fiz. **69** (10), 51 (1999) [Tech. Phys. **69**, 1175 (1999)].
18. V. V. Lasukov and T. V. Fursa, Pis'ma Tekh. Fiz. **26** (6), 36 (2000) [The. Phys. Lett. **26**, 241 (2000)].
19. V. N. Mineev and A. G. Ivanov, Usp. Fiz. Nauk **119** (1), 75 (1976) [Sov. Phys. Usp. **19**, 400 (1976)].
20. M. E. Perel'man and N. G. Khatiashvili, Dokl. Akad. Nauk SSSR **256**, 824 (1981) [in Russian].
21. Ya. I. Frenkel', Zh. Fiz. Khim. **14**, 305 (1940).
22. M. A. Margulis, Usp. Fiz. Nauk **170**, 263 (2000) [Phys. Usp. **43**, 259 (2000)].
23. Y. Kawawuchi, X. Ding, A. Narazaki, et al., Appl. Phys. A **80**, 275 (2005).